ISSN 0202-2893, Gravitation and Cosmology, 2026, Vol. 32, No. 2, pp. 314–332. © Pleiades Publishing, Ltd., 2026.

Relaxation in Scalar Gravitational Field Theory

Riccardo Fantoni*

Università di Trieste, Dipartimento di Fisica, strada Costiera 11, Grignano (Trieste), 34151 Italy

Received February 7, 2025; revised June 10, 2025; accepted October 15, 2025

Abstract—We revisit the problem of relaxation in a scalar gravitational field theory proposing a novel numerical solution to the problem. We predict the approach to equilibrium of a spherically symmetric field-particle system initially excited in a non-equilibrium state, where the particle is in an unstable circular orbit around the origin. We explicitly work out a quasistatic approximation in an unstable circular orbit to the exact dynamical problem. Our toy model could give some relevant insights in the full General Relativity realistic model as theoretical effort is carried on to solve it numerically. For example we propose to use the method of images to tackle a numerical solution of the resulting wave equation.

DOI: 10.1134/S020228932670012X

1. INTRODUCTION

In this work we want to predict the approach to equilibrium of a spherically symmetric field-particle system initially excited in a non-equilibrium state, where the particle is in an unstable circular orbit around the origin [1]. This toy model could give some relevant insights in the full General Relativity (GR) realistic model, as theoretical effort is carried on to solve it numerically.

In particular we will be concerned with realization of a quasistatic approximation to the exact dynamical problem. As the newly built gravitational wave detectors are preparing to receive their first set of data, theoretical effort is applied to exactly solve Einstein's equation to be able to timely interpret such data. Our quasistatic approximation in an unstable circular orbit of our toy model could become an important tool in the event that such theoretical effort fails to solve the realistic GR problem in time. The approximation should be particularly useful in interpreting the waveform coming from slowly decaying binary neutron stars.

Binary neutron stars are known to exist, and for some of the systems in our own galaxy (like the relativistic binary radio pulsars PSR B1913+16 and PSR B1534+12), GR effects in the binary orbit have been measured to high precision. With the construction of laser interferometers well underway, it is of growing urgency that we be able to predict theoretically the gravitational waveform emitted during the inspiral and the final coalescence of two stars. Relativistic binary systems like binary neutron stars and binary black holes pose a fundamental challenge to theorists, as the two-body problem is one of the outstanding unsolved problems in classical GR.

When studying a two-body problem, one decomposes it to a trivial problem involving the center of mass motion and a harder one involving the relative motion of the two masses. It is the second one that we want to focus on. Since we do not want to deal with all difficulties of GR (there is no analytic solution to the two body problem in GR), and we want to have a more realistic theory than the Newtonian one, we choose to employ a theory which describes gravitation by a nonlinear scalar gravitational field Φ in special relativity. To describe the relative motion in a two body problem, we just need one particle moving around the origin. The particle motion is confined at all times in its orbital plane, and its position there is determined by the distance from the origin r_p, and the azimuthal angle ϕ_p. To follow the dynamical evolution of the field-particle system in scalar gravity, one needs to solve a single hyperbolic partial differential equation describing the field evolution, coupled to a system of two ordinary differential equations describing the particle motion,

$$\begin{aligned} \Box\Phi(\mathbf{r},t) &= \text{source},\\ \ddot{r}_p &= \dots,\\ \ddot{\phi}_p &= \dots. \end{aligned} \tag{1}$$

The source term of the field equation is where a coupling between the field and the particle dynamics takes place, and it is responsible for the nonlinearity of the problem: source $\sim \exp(\Phi)\rho$, where $\rho(\mathbf{r},t) = (m/\gamma)\delta(\mathbf{r}-\mathbf{r}_p(t))$ is the comoving matter density, m the particle rest mass, and γ the Lorentz factor.

*E-mail: riccardo.fantoni@scuola.istruzione.it

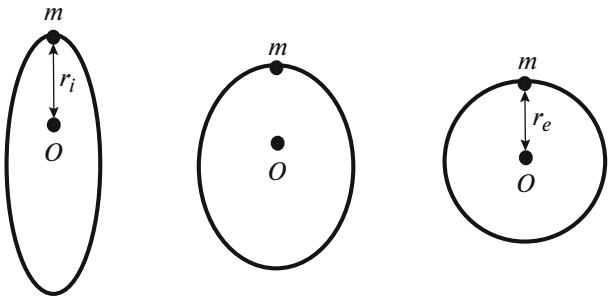

Fig. 1. Pictorial evolution of the particle orbit when $J > 1$.

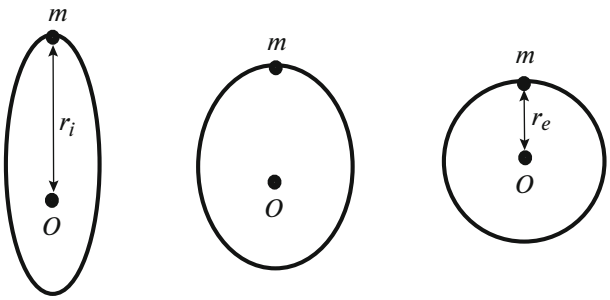

Fig. 2. Pictorial evolution of the particle orbit when $J < 1$.

In particular, we want to study an even simpler, spherically symmetric problem. It is in fact a peculiarity of scalar gravitation, that of being able to generate gravitational waves even in spherical symmetry. This allows a study of wave generation and propagation with the use of just one spatial dimension plus time. In spherical symmetry, the particle angular momentum $\tilde{u}_\phi$ is conserved. There are then three important quantities in our problem: the initial distance from the origin r_i, the particle rest mass m, and its angular momentum $\tilde{u}_\phi$. Two adimensional combinations of these quantities are particularly important to parametrize the problem:

(1) The initial compaction $\alpha = r_i/m$ which tunes the nonlinearity of the problem:

- $\alpha \gg 1$ The system is in a weak field and slow particle velocity regime. Newtonian gravitation provides a good analytic approximation to the nearly linear and periodic system.
- $\alpha \sim 1$ The system is nonlinear and aperiodic. There is no analytic solution to the coupled equations (1), and numerical integration is needed. In this paper we will describe an approximate solution which works well when the system relaxes slowly.

(2) An adimensional measure of the particle angular momentum $J = \tilde{u}_\phi/(\tilde{u}_\phi)_{\rm circ}(r_i)$. Here we are indicating with $(\tilde{u}_\phi)_{\rm circ}(r_i)$ the angular momentum that the particle should have in order to be in a circular orbit at the initial radius r_i.

- $J = 0$ The particle collapses to the origin.
- $J = 1$ The particle is in a stable circular orbit. Even though the particle is in circular motion around the origin, it does not lose energy by gravitational radiation because in spherical symmetry a particle in circular orbit represents a stationary spherical mass shell.
- $J > 1$ The particle is initially at the periastron of its elliptical orbit. There is a value J_e such that if $J > J_e$, the particle escapes to infinity, if $J < J_e$ the particle orbit becomes circular at $t = \infty$, of radius r_e larger than r_i.
- $J < 1$ The particle is initially at the apastron of its elliptical orbit. The particle orbit becomes circular at $t = \infty$, of radius r_e smaller than r_i. If $J \ll 1$, the shell relaxation will be fast (it will reach r_e in a small number of oscillations), and the quasistatic approximation that we are now going to describe will break down.

When the timescale of orbital decay by radiation is much longer than the orbital period, the particle can be considered to be in "quasiequilibrium." When this condition is satisfied, we are allowed to drop the $\Phi_{,tt}$ (radiative) term from the field equation. Doing this, the problem reduces to the solution of three ordinary differential equations, which can be solved "analytically." We will call this simpler problem the "static" approximation to the exact problem,

$$\begin{aligned} \nabla^2\Phi &= \text{source}, \\ \ddot{r}_p &= \dots, \\ \ddot{\phi}_p &= \dots . \end{aligned} \tag{2}$$

In the static approximation (which reduces to Newtonian gravity in the limit $\alpha \gg 1$), the particle motion is conservative but not necessarily periodic due to nonlinearity of the problem.

Monitoring the exact solution for the field at a fixed radius $r_{\rm out}$ far from the particle, one expects a behavior similar to the one shown in Fig. 3.

In particular, damping of the wave amplitude is due to the fact that the particle is gradually approaching a circular orbit. In the static approximation, the

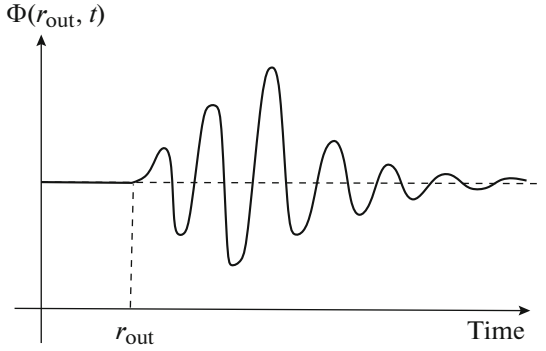

Fig. 3. The expected behavior for $\Phi(r_{\rm out}, t)$ as a function of time.

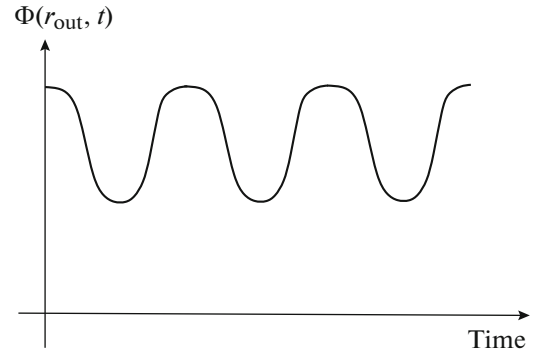

Fig. 4. The same as Fig. 3 but in the static approximation.

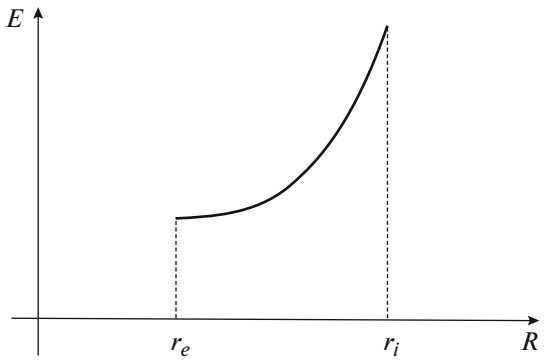

Fig. 5. The expected behavior of the total energy E of the system as a function of the circular orbits radius R. The energy curve has its minimum at r_e, the radius of the circular orbit on which the particle decays at $t = \infty$.

field cannot have any damping due to conservativity of the particle motion, and we get a behavior shown in Fig. 4.

Any reasonable approximation to the exact solution in the nonlinear regime must be able to reproduce damping of the wave. The "quasistatic" approximation that we propose takes into account the wave damping through the following four steps:

(1) We use the solution $r_p(t)$ in the static approximation to determine the field equation source term. We then solve the full field equation,

$$\Box\Phi(\mathbf{r}, t) = \text{source} \tag{3}$$

to find the flux of field energy ($\sim r^2\Phi_{,t}\Phi_{,r}$) radiated out by the gravity wave. This will allow us to determine changing rate of the total energy E of the particle-field system with respect to time,

$$\frac{dE}{dt} = -\int \text{flux}\, da. \tag{4}$$

(2) Consider the particle-field system in a stationary state where the particle is in a circular orbit at a radius R. Then instantaneously change the particle angular momentum from $J = 1$ to $J = \tilde{u}_\phi/(\tilde{u}_\phi)_{\rm circ}(R)$ and calculate the total energy of the system. Repeating this for all radii R between r_i and r_e, we get a curve $E(R)$ similar to the one shown in Fig. 5. The values $E(r_e)$ and $E(r_i)$ are exact, while at the true inversion points $r_{\rm inv}$ of the particle orbit, $E(r_{\rm inv})$ are expected to be good approximations to the corresponding exact values. Knowing $E(R)$, we can find the changing rate of E with respect to R.

(3) Use the chain rule to get the rate of change of R in time,

$$\frac{dR}{dt} = \frac{dE/dt}{dE/dR}. \tag{5}$$

(4) Finally, knowing dR/dt, we can correct the previous static estimate of the field equation source term. We can then solve the full field equation again to get the wave damping.

2. STATEMENT OF THE PROBLEM

2.1. Basic Equations

The gravitational field is described by a massless scalar field $\Phi(x^\alpha)$ in special relativity. The scalar field does not modify the background space-time geometry which is always Minkowskian. Consider a particle of rest mass m moving along a world line $z^\alpha(\lambda)$. Then the action for the field-particle system is

$$I = \int \mathcal{L}\,(-g)^{1/2}\, d^4x, \tag{6}$$

where the Lagrangian density $\mathcal{L}$ is

$$\mathcal{L} = -\frac{1}{8\pi G}\, g^{\alpha\beta}\Phi_{,\alpha}\Phi_{,\beta} - \rho e^{\Phi}, \tag{7}$$

and where the comoving density is

$$\rho = m \int \left(-g_{\alpha\beta} \frac{dz^\alpha}{d\lambda} \frac{dz^\beta}{d\lambda} \right)^{1/2} \times \delta^4(\vec{x} - \vec{z}(\lambda)) \, (-g)^{-1/2} \, d\lambda. \quad (8)$$

Here, the metric tensor $g_{\alpha\beta}$ is the usual Minkowski metric $\eta_{\alpha\beta}$ since space-time is flat in this theory (i.e., $g_{\alpha\beta} = \eta_{\alpha\beta} = \mathrm{diag}(-1,1,1,1)$ in Cartesian coordinates), and $g = \det\{g_{\mu\nu}\} = -1$. We use arrows to denote four-vectors and boldface to denote three-vectors. We will set the speed of light $c = 1$, but will display the gravitational coupling constant (Newton's constant) G explicitly. If we choose λ equal to proper time τ along the particle world-line, then

$$\rho = m \int \delta^4(\vec{x} - \vec{z}(\tau)) \, (-g)^{-1/2} \, d\tau \quad (9)$$

$$= \frac{m}{\gamma} \delta^3(\mathbf{x} - \mathbf{z}(t)) \, (-g)^{-1/2}, \quad (10)$$

where $\gamma \equiv dz^0/d\tau$ is the Lorentz factor.

Varying the Lagrangian (7) with respect to Φ gives the field equation

$$\Box\Phi = 4\pi G e^{\Phi} \rho. \quad (11)$$

In the Newtonian limit, where $\Phi \ll 1$, Eq. (11) becomes linear and reduces to Poisson' s equation. Varying the Lagrangian with respect to z^α gives the particle equation of motion

$$\frac{D^2 z^\alpha}{d\tau^2} + \left[g^{\alpha\beta} + \frac{dz^\alpha}{d\tau} \frac{dz^\beta}{d\tau} \right] \Phi_{,\beta} = 0, \quad (12)$$

where D denotes covariant differentiation. Here we are allowing for curvilinear coordinates, while covariant differentiation reduces to ordinary differentiation in Cartesian coordinates. In the nonrelativistic limit, Eq. (12) implies that the gravitational force is $-\nabla\Phi$. The fully relativistic form ensures that the four-velocity $u^\alpha = dz^\alpha/d\tau$ remains orthogonal to the four-acceleration $a^\alpha = Du^\alpha/d\tau$ (in fact, $u_\alpha u^\alpha = -1$).

2.2. The Problem

Since scalar gravitation can generate gravitational waves in spherical symmetry, we can test out computational algorithms for calculating gravitational radiation on *one-dimensional* systems. This is much simpler than in GR. While not every aspect of the GR problem is reflected in this setting, many features of wave generation in a rapidly varying nonlinear dynamical system are exhibited here.

Consider one particle of rest mass m moving along a world line $z^\alpha(\tau) = (\mathbf{r}_p, t)$ with four-velocity u^α, under the influence of a massless scalar gravitational field $\Phi(\mathbf{r}, t)$ in special relativity. In spherical symmetry, the comoving matter density takes the form

$$\rho(r,t) = \frac{m/\gamma}{4\pi r_p^2(t)} \delta(r - r_p(t)), \quad (13)$$

where $r = |\mathbf{r}|$, and $\gamma = u^0$ is the Lorentz factor. The particle effectively represents an entire spherical shell of radius r_p and mass surface density $\sigma = m/(\gamma 4\pi r_p^2)$.

Assuming the particle confined in the $\theta = \pi/2$ plane, so that $u^\theta = 0$ at all times, the equations of motion in spherical coordinates $\mathbf{r}_p = (r_p, \theta_p, \phi_p)$, are (see Appendix 7),

$$\dot{r}_p = \frac{\tilde{u}_r}{\tilde{u}^0}, \quad \dot{\tilde{u}}_r = \frac{\tilde{u}_\phi^2}{\tilde{u}^0 \, r_p^3} - \frac{e^{2\Phi}\Phi_{,r}}{\tilde{u}^0},$$

$$r_p^2 \dot{\phi}_p = \frac{\tilde{u}_\phi}{\tilde{u}^0}, \quad \dot{\tilde{u}}_\phi = 0, \quad (14)$$

$$\tilde{u}^0 = \sqrt{e^{2\Phi} + \tilde{u}_r^2 + \tilde{u}_\phi^2/r_p^2}, \quad (15)$$

$$\tilde{u}^\alpha \equiv e^{\Phi} u^\alpha, \quad (16)$$

where the dot stands for a time derivative, and we use commas to indicate partial differentiation.

The particle moves conserving its orbital angular momentum $\tilde{u}_\phi$. In a static gravitational field, the particle energy $\tilde{u}^0$ is also constant.

Notice that from the field equation (11) it follows that $\phi_{,r}$ has, at all times,[1] a jump of $4\pi G e^{\Phi}\sigma$ on the shell surface $r = r_p(t)$. It is then necessary to specify how we calculate the gravitational force felt by the shell. We will use in equation (14),

$$\Phi_{,r} \equiv [\Phi_{,r}(r_p-) + \Phi_{,r}(r_p+)]/2. \quad (17)$$

In this way we prevent any small patch of surface on the shell from interacting with itself.

2.3. Initial Condition

The field starts from a moment of time symmetry, so that at $t = 0$,

$$\Phi_{,t} = 0, \quad \nabla^2\Phi = 4\pi G e^{\Phi} \sigma \delta(r - r_i),$$

where $r_i = r_p(t = 0)$ is the initial shell radius. The field is subject to the boundary conditions

$$\Phi_{,r} = 0, \quad r = 0; \quad (18)$$

$$(r\Phi)_{,r} = 0, \quad r \to \infty. \quad (19)$$

Choosing

$$\Phi = \begin{cases} a/r_p, & r \le r_p \\ a/r, & r > r_p, \end{cases} \quad (20)$$

[1] We can safely assume that $\Phi_{,tt}$ remains finite at all times on the shell surface.

we can determine $a_i = a(t=0)$ from the matching condition at the shell surface,

$$\Phi_{,r}(r_p+) - \Phi_{,r}(r_p-) = \frac{Gm\, e^{2\Phi}}{r_p^2 \tilde{u}^0}. \tag{21}$$

Initially, the particle is in a circular orbit of radius r_i around the origin,

$$\tilde{u}_r = 0,$$
$$r_i (u^\phi_{\rm circ})^2 = [\Phi_{,r}(r_i-) + \Phi_{,r}(r_i+)]/2 = -\frac{a_i}{2r_i^2}, \tag{22}$$

with the angular momentum

$$(\tilde{u}_\phi)_{\rm circ} = e^\Phi r_i^2 u^\phi_{\rm circ} = e^{a_i/r_i}\sqrt{-\frac{a_i r_i}{2}}. \tag{23}$$

We can then find a_i from Eq. (22), which becomes

$$a_i = -\frac{Gm\, e^{a_i/r_i}}{\sqrt{1 - a_i/(2r_i)}}. \tag{24}$$

This initial condition (an Einstein state) is a stationary wave for the field equation of motion and a stable circular orbit for the particle. So if we let the system evolve from this initial state, nothing will happen: the particle will keep moving in the circular orbit at radius $r_p(t) = r_i$ under the influence of the static gravitational field (20). This can be shown, for example, by rewriting the field equation in terms of the auxiliary functions,

$$X(r,t) = [(r\Phi)_{,r} + (r\Phi)_{,t}]/2,$$
$$Y(r,t) = [(r\Phi)_{,r} - (r\Phi)_{,t}]/2. \tag{25}$$

Now Eq. (11) becomes

$$X_{,t} = X_{,r} - F\delta(r - r_p),$$
$$Y_{,t} = -Y_{,r} + F\delta(r - r_p), \tag{26}$$

where $F = Gm\exp(2\Phi)/(2r_p\tilde{u}^0)$. The initial condition for X and Y becomes

$$X(r,0) = 0,$$
$$Y(r,0) = \begin{cases} a_i/(2r_i) & -r_i < r < r_i \\ 0 \quad \text{otherwise.} \end{cases} \tag{27}$$

From Eqs. (23) and (24) it follows that when $\tilde{u}_\phi/(\tilde{u}_\phi)_{\rm circ} = 1$, at $t = 0$, the source term is $F = a_i/(2r_i)$, so that after an infinitesimal time step dt, $X(r, dt) = X(r, 0)$, and $Y(r, dt) = Y(r, 0)$.

So we perturb the system changing the particle' s angular momentum by a factor ξ,

$$\tilde{u}_\phi = \xi\ (\tilde{u}_\phi)_{\rm circ}, \tag{28}$$

and let it evolve.

2.4. Conserved Integrals

The particle-field dynamical system is characterized by a time-varying matter and velocity profile, interacting with a time-varying scalar field containing radiation. Conservation of energy-momentum follows from

$$\nabla T = 0, \tag{29}$$

where T is the total stress-energy tensor of the system,

$$T^{\mu\nu} = \frac{2}{(-g)^{1/2}}\frac{\delta[\mathcal{L}(-g)^{1/2}]}{\delta g_{\mu\nu}}. \tag{30}$$

Carrying out variation using Eq. (7), we find,

$$T_{\mu\nu} = T^{\rm field}_{\mu\nu} + T^{\rm particle}_{\mu\nu}, \tag{31}$$

where

$$T^{\rm field}_{\mu\nu} = \frac{1}{4\pi G}[\Phi_{,\mu}\Phi_{,\nu} - \frac{1}{2}g_{\mu\nu}\Phi^{,\alpha}\Phi_{,\alpha}], \tag{32}$$
$$T^{\rm particle}_{\mu\nu} = \rho e^\Phi u_\mu u_\nu. \tag{33}$$

Conservation of energy-momentum gives rise to the following conserved integrals:

$$\frac{\partial}{\partial t}\int_{S_r} T^{\mu 0}(\mathbf{x},t)\, d^3x = -\int T^{\mu i}{}_{,i}\, d^3x$$
$$= -4\pi r^2 T^{\mu r}(r,t), \tag{34}$$

where S_r is the volume of a sphere of radius r centered at the origin, and we have used spherical symmetry in the last equality.

When $r > r_p(t)$, we find

$$[\mu = 0] \quad \frac{\partial}{\partial t}\left\{\frac{1}{2G}\int_0^r [(\Phi_{,0})^2 + (\Phi_{,r})^2] r^2 dr + m\tilde{u}^0\right\}$$
$$= \frac{1}{G} r^2 \Phi_{,0}\Phi_{,r},$$
$$[\mu = \phi] \quad \frac{\partial}{\partial t}\left(\frac{\tilde{u}_\phi}{r_p^2}\right) = 0,$$
$$[\mu = r] \quad \frac{\partial}{\partial t}\left\{\frac{1}{G}\int_0^r \Phi_{,0}\Phi_{,r} r^2\, dr - m\tilde{u}_r\right\}$$
$$= \frac{1}{2G} r^2 [(\Phi_{,0})^2 + (\Phi_{,r})^2]. \tag{35}$$

The particle-field total mass-energy is given by the integral in Eq. (35),

$$E = E^{\rm field} + E^{\rm particle},$$
$$E^{\rm field} = \frac{1}{2G}\int_0^r [(\Phi_{,0})^2 + (\Phi_{,r})^2] r^2\, dr,$$

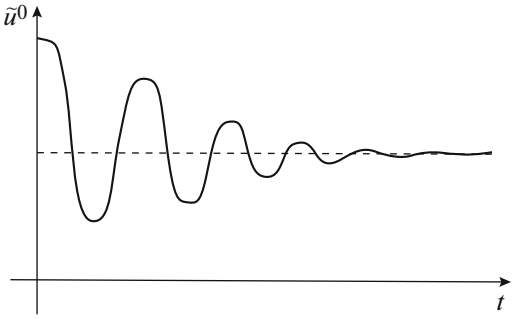

Fig. 6. The expected behavior of the particle energy $\tilde{u}^0$ as a function of time for the case $\alpha \sim 1$ and $\xi < 1$.

$$E^{\text{particle}} = m\tilde{u}^0. \tag{36}$$

According to Eq. (35), when evaluated at large enough radius outside any radiation or matter, E is conserved. As the particle shell breaths around its asymptotic virial equilibrium state, E^{particle} undergoes exponentially dumped oscillations around its asymptotic value (see Fig. 6): the oscillations are due to coupling with the field, and dumping to gravitational radiation going out to infinity (as a gravity wave). Thus after a long time, apart from some particular combinations of ξ and r_i/m (see Subsection 2.7), some energy will have been exchanged between the field and the particle.

For a static situation, the term $(\Phi_{,r})^2$ in Eq. (36) can be integrated by parts to get

$$E = -\frac{m\Phi_p e^{2\Phi_p}}{2\tilde{u}^0} + m\tilde{u}^0, \tag{37}$$

where $\Phi_p = \Phi(r_p, t)$. In the Newtonian limit, Eq. (37) becomes

$$\begin{aligned} E &= m\Big[-\frac{\Phi_p}{2} + \cdots + (1 + \Phi_p + \cdots) \\ &\quad \times \Big(1 + \frac{v_r^2}{2} + \frac{v_\phi^2}{2r^2} + \cdots\Big)\Big] \\ &\approx m\Big(1 + \frac{v_r^2}{2} + \frac{v_\phi^2}{2r^2} + \frac{\Phi_p}{2}\Big), \end{aligned} \tag{38}$$

where $v_i \equiv u_i/u^0$. So E is a sum of the rest mass plus kinetic energy plus gravitational potential energy of the matter shell.

When $r < r_p(t)$,

$$[\mu = 0] \quad \frac{\partial}{\partial t}\int_0^r [(\Phi_{,0})^2 + (\Phi_{,r})^2] r^2\, dr = 2r^2\Phi_{,0}\Phi_{,r},$$

$$[\mu = \phi] \quad 0 = 0,$$

$$[\mu = r] \quad \frac{\partial}{\partial t}\int_0^r \Phi_{,0}\Phi_{,r} r^2 dr = \frac{r^2}{2}[(\Phi_{,0})^2 + (\Phi_{,r})^2], \tag{39}$$

which implies

$$(\Phi_{,0})^2 = (\Phi_{,r})^2, \quad \forall t, \quad \forall r < r_p(t). \tag{40}$$

Those conserved integrals can be used as self-consistent checks on our numerical integration. In Fig. 7 we show what we would expect if we were to evaluate the energy conservation equation,

$$\begin{aligned} &\int_0^{r_{\text{ec}}} [(\Phi_{,0})^2 + (\Phi_{,r})^2] r^2\, dr + 2m\tilde{u}^0\theta(r_{\text{ec}} - r_p(t)) \\ &\quad - 2\int_0^t dt[\Phi_{,0}\Phi_{,r} r_{\text{ec}}^2 - m\delta(r_{\text{ec}} - r_p(t))\tilde{u}_r] \\ &\quad = b\int_0^{r_{\text{ec}}} (\Phi(r,0)_{,r} r)^2 dr \\ &\quad + 2m\tilde{u}^0\big|_{t=0}\theta(r_{\text{ec}} - r_p(0)), \end{aligned} \tag{41}$$

as a function of time at two fixed radii r_{ec}. The first radius is inside the shell at all times, the second one is always in the vacuum exterior. In the first case, the right-hand side of Eq. (41) is zero, the integrated flux term (the second integral in Eq. (41)) is large, and the energy conservation involves cancellation of large terms. Consequently, the high degree to which we are able to maintain energy conservation is a nontrivial measure of the code accuracy. In the exterior, the flux is small, and energy conservation is not a stringent test.

2.5. Monopole Radiation

In the weak field, slow motion limit, the radiation field can be obtained by a multipole expansion. Since the theory involves a scalar field, the lowest-order contribution to radiation comes from the monopole term. This is in contrast to electromagnetism (vector field: dipole radiation) or GR (tensor field: quadrupole radiation).

Using Green' s function for the wave equation, we can transform Eq. (11) to an integral form,

$$\Phi(\mathbf{x}, t) = -G\int d^3x' \frac{\big[e^{\Phi}\rho\big]_{t'=t-|\mathbf{x}-\mathbf{x}'|}}{|\mathbf{x} - \mathbf{x}'|}. \tag{42}$$

In the wave zone, we can replace the denominator in Eq. (42) with the distance $r = |\mathbf{x}|$. To isolate the conserved rest mass m, define the rest density as

$$\rho_0 = \gamma\rho. \tag{43}$$

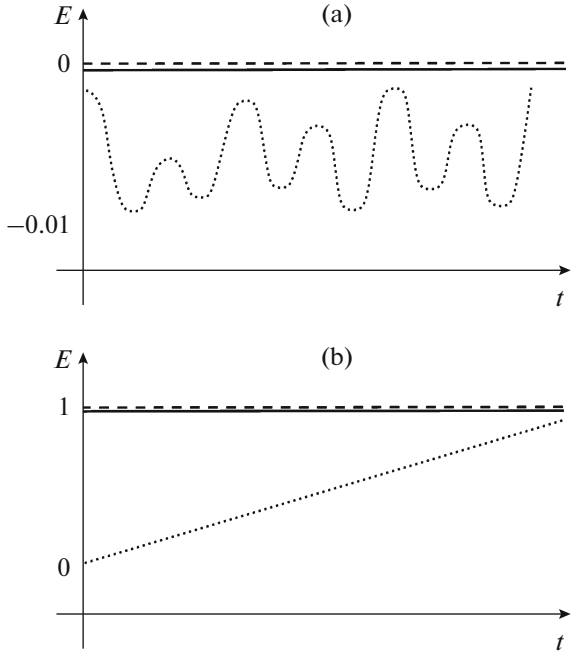

Fig. 7. Energy conservation at two selected radii as a function of time. The solid line shows the left-hand side of Eq. (41) (volume integral plus integrated flux), the dotted line shows the second term alone (integrated flux), and the dashed line shows the right-hand side (volume integral at $t = 0$). The radii are (a) $r_{\rm ec} < r_p(t)$ at all times, (b) $r_{\rm ec} > r_p(t)$ at all times. The degree to which the solid and dashed lines coincide compared with the magnitude of the dotted line is a measure of the code' s ability to conserve energy.

Then,

$$\Phi(\mathbf{x},t) \approx -\frac{G}{r}\int d^3x' \left[\frac{e^\Phi}{\gamma}\rho_0\right]_{t'=t-|\mathbf{x}-\mathbf{x}'|}. \qquad (44)$$

In the integrand, expand

$$\rho_0(\mathbf{x}',t') = \rho_0(\mathbf{x}',t-r) + (r-|\mathbf{x}-\mathbf{x}'|)\rho_{0,t} + \tfrac{1}{2}(r-|\mathbf{x}-\mathbf{x}'|)^2\rho_{0,tt} + \cdots, \qquad (45)$$

and

$$\frac{e^\Phi}{\gamma} = [1+\Phi-\tfrac{1}{2}v^2]_{t'=t-r} + \cdots, \qquad (46)$$

where $v^2 = [u_r/u^0]^2 + [u_\phi/(u^0 r)]^2$. At large r,

$$r - |\mathbf{x}-\mathbf{x}'| \approx \frac{\mathbf{x}\cdot\mathbf{x}'}{r} = r'\cos\theta'. \qquad (47)$$

The leading-order contribution to the expansion of Eq. (44) comes from the product of ρ_0 in Eq. (45) with the "1" in Eq. (46). The resulting integral gives m, so that this term represents the nonradiative Coulomb field. Thus the leading-order radiation field is

$$\Phi(\mathbf{x},t) = -\frac{G}{r}\int d^3x'[\rho_0(\Phi-\tfrac{1}{2}v^2) + r'\cos\theta'\rho_{0,t} + r'^2\cos^2\theta'\rho_{0,tt}]_{\,t-r}. \qquad (48)$$

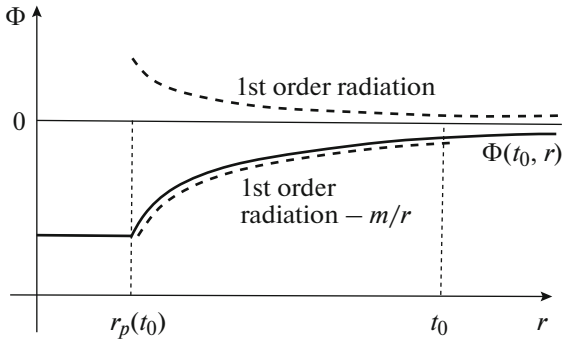

Fig. 8. For the case $\alpha \sim 1$, $\xi < 1$, a snapshot at $t = t_0$ of the field $\Phi(t_o, r)$, the first-order radiation part (52), and the first-order radiation part plus the zero-order $-m/r$.

To this order, it is irrelevant whether one uses ρ or ρ_0 in Eq. (48).

For a spherically symmetric density distribution, the term proportional to $\cos\theta'$ in Eq. (48) integrates to zero, giving

$$\Phi(r,t) = -\frac{G}{r}\int dr'\,4\pi r'^2[\rho_0(\Phi-\tfrac{1}{2}v^2) + \tfrac{1}{6}r_p^2\rho_{0,tt}]_{t-r}. \qquad (49)$$

The last term in the integrand can be rewritten as follows:

$$\frac{1}{6}\int dr'\,4\pi r'^2\frac{d^2(r'^2)}{dt^2}\rho_0 = \frac{1}{3}m\left(\tilde{u}_r^2 + r_p\frac{d\tilde{u}_r}{dt}\right), \qquad (50)$$

and using the equation of motion (14) in the weak field limit, we find

$$\frac{1}{6}\int dr' 4\pi r'^2\frac{d^2(r'^2)}{dt^2}\rho_0 = \frac{m}{3}\left(\tilde{u}_r^2 + \frac{\tilde{u}_\phi^2}{r_p^2} - r_p\Phi_{,r}\right). \qquad (51)$$

Thus Eq. (49) becomes

$$r\Phi(r,t) = Gm\left\{\frac{1}{6}\left[r_p(\Phi_{,r}(r_p+) + \Phi_{,r}(r_p-)) + \tilde{u}_r^2 + \frac{\tilde{u}_\phi^2}{r_p^2}\right] - \Phi\right\}_{t-r}. \qquad (52)$$

Figure 8 shows how a snapshot of the field at $t = t_o$ should look like and compare it with the leading-order radiation field of Eq. (52), in the wave zone.

From Eq. (35) it follows that the energy emission rate when $r > r_p(t)$ is

$$\frac{dE}{dt} = -\frac{1}{G}r^2\Phi_{,t}\Phi_{,r} = -\frac{1}{G}(r\Phi_{,t})^2, \qquad (53)$$

where, in the last equality, we used the fact that since X is propagating to the left, the following outgoing wave boundary condition must hold:

$$X(r,t)=0, \quad \text{or} \quad (r\Phi)_{,r}+(r\Phi)_{,t}=0, \\ \forall t, \quad \forall r > r_p(t). \tag{54}$$

2.6. Analytic Results

Newtonian limit. For weak fields and slow velocities we can test our code using the analytic solution from Newtonian gravitation. In this limit, the particle equation of motion is

$$\ddot{r_p}=-\Phi_{,r}+\frac{J^2}{r_p^3}, \\ \Phi_{,r}=\frac{Gm}{2\,r^2}, \quad J=(r^2 v_\phi)_{t=0} \\ =r_i^2\xi\sqrt{\Phi_{,r}(r_i)/r_i}=\xi\sqrt{Gmr_i/2}, \tag{55}$$

which can be rewritten as

$$\ddot{x}=-\frac{M_{\text{eff}}}{x^2}+\frac{J_{\text{eff}}^2}{x^3}, \\ \dot{x}(0)=0, \quad x(0)=1, \tag{56}$$

where $r_p(t)=r_i x(t)$, $M_{\text{eff}}=Gm/(2r_i^3)$, and $J_{\text{eff}}=\xi\sqrt{M_{\text{eff}}}$. The first integral yields the conserved energy

$$E=\frac{1}{2}\dot{x}^2-\frac{M_{\text{eff}}}{x}+\frac{J_{\text{eff}}^2}{2x^2}. \tag{57}$$

For $E=M_{\text{eff}}(\xi^2/2-1)<0$ (i.e., $\xi^2<2$) we have bound orbits. Solving for the turning points ($\dot{x}=0$) yields

$$x_+=\frac{1\pm(1-\xi^2)}{2-\xi^2}, \tag{58}$$

so that at $0<\xi<1$ the shell contracts to $r_i x_-$, and for $1<\xi<\sqrt{2}$ it expands to $r_i x_-$. At $\xi>\sqrt{2}$ the shell explodes.

Integrating the equation of motion, we get the parametric solution

$$x=a(1-e\cos(u)), \\ t=\frac{P}{2\pi}(u-e\sin(u))-\frac{P}{2}, \tag{59}$$

where the semimajor axis, eccentricity and period are given by

$$a=\frac{1}{2-\xi^2}, \quad e=|1-\xi^2|, \\ P=2\pi\sqrt{\frac{2r_i^3}{Gm(2-\xi^2)^3}}. \tag{60}$$

Inserting this analytic solution into Eq. (49) and differentiating with respect to time gives the wave amplitude in the wave zone

$$r\Phi_{,t}=-\frac{4}{3}\frac{(Gm)^2}{r_i}\left[\frac{\dot{x}}{x^2}\right]_{t-r}. \tag{61}$$

From Eq. (53) we get for the energy emission rate

$$\frac{dE}{dt}=-\frac{16}{9}\frac{(Gm)^4}{r_i^2}\left[\frac{\dot{x}^2}{x^4}\right]_{t-r}. \tag{62}$$

Integrating over an oscillation period, we get the energy radiated per period,

$$\Delta_P E=-\frac{16\pi}{36}m\left(\frac{Gm}{r_i}\right)^{7/2} \\ \times\frac{(1-\xi^2)^2}{\xi^7}(5-2\xi^2+\xi^4). \tag{63}$$

2.7. Relaxation to Virial Equilibrium

If the shell does not explode or collapse, it will eventually reach, as it loses energy by emitting gravitational waves, an equilibrium circular orbit (see Fig. 9). At this point, the particle-field system is in an Einstein state where $\tilde{u}_r=0$, $\tilde{u}_\phi^2=r_p^3 e^{2\Phi}\Phi_{,r}$, and the field is static and of the form (20), in a neighborhood of the shell.

Given the particle's angular momentum $\tilde{u}_\phi$, we can predict the final equilibrium radius r_e by solving the following equations in $a_e=a(t=\infty)$ and $r_e=r_p(t=\infty)$:

$$a_e=-\frac{Gm\,e^{2a_e/r_e}}{\sqrt{e^{2a_e/r_e}+\tilde{u}_\phi^2/{r_e}^2}}, \tag{64}$$

$$\tilde{u}_\phi^2=e^{2a_e/r_e}{r_e}^3(-a_e/(2{r_e}^2)). \tag{65}$$

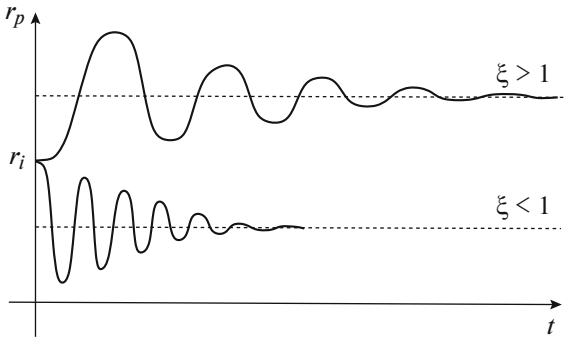

Fig. 9. Relaxation to the virial equilibrium state for an $\alpha\sim 1$ shell with two different values of ξ: $\xi<1$ and $\xi>1$.

One can verify that

$$\begin{cases} r_e < r_i & \text{if} \quad \xi < 1 \\ r_e > r_i & \text{if} \quad \xi > 1. \end{cases} \tag{66}$$

This final state is a virial equilibrium state. Taking the trace of the special-relativistic virial theorem

$$\int T^{ij} d^3x = \frac{1}{2} \frac{\partial^2}{\partial t^2} \int T^{00} x^i x^j d^3x \tag{67}$$

gives at equilibrium

$$\int \rho e^{\Phi} ({u_r}^2 + {u_\phi}^2/r^2) d^3x$$
$$= \frac{1}{8\pi G} \int (\nabla\Phi)^2 d^3x = -\frac{1}{2} \int \rho \Phi e^{\Phi} d^3x, \tag{68}$$

or, at $\tilde{u}_r = 0$,

$$\frac{\tilde{u}_\phi^2}{r_e^2} = -\frac{1}{2} e^{2\Phi} \Phi, \tag{69}$$

which is the same as Eq. (65) when the field is of the form (20).

The final energy of the particle-field system is

$$E\Big|_{t=\infty} = -\frac{m}{2} \frac{a}{r_e} \frac{e^{2a/r_e}}{\tilde{u}^0\big|_{t=\infty}} + m\tilde{u}^0\Big|_{t=\infty}, \tag{70}$$

where

$$\tilde{u}^0(t=\infty) = \sqrt{e^{2a_e/r_e} + \tilde{u}_\phi^2/r_e^2}. \tag{71}$$

The shell will only collapse into the origin if it possesses zero angular momentum.[2] It follows from Eq. (15) and the observation that the particle energy $m\tilde{u}^0$ is always smaller than the initial total energy of the particle-field system $E(t=0)$. Since the exponential is positive, we can write

$$[E(t=0)]^2 > \tilde{u}_r^2 + \frac{\tilde{u}_\phi^2}{r^2}, \tag{72}$$

and if $\tilde{u}_r = 0$, Eq. (72) gives the following lower bound on the accessible radii:[3]

$$r_p > \tilde{u}_\phi / E\Big|_{t=0}, \tag{73}$$

where

$$E\Big|_{t=0} = \frac{a^2}{2r_i} + m\tilde{u}^0\Big|_{t=0},$$
$$\tilde{u}^0\Big|_{t=0} = \sqrt{e^{2a/r_i} + \tilde{u}_\phi^2/r_i^2}. \tag{74}$$

[2] It is different from what happens in GR where a shell can also collapse with nonzero values of the angular momentum.

[3] At sufficiently small ξ one can get a better lower bound by substituting $E(t=0)$ with $\tilde{u}^0(t=0)$ in Eq. (73).

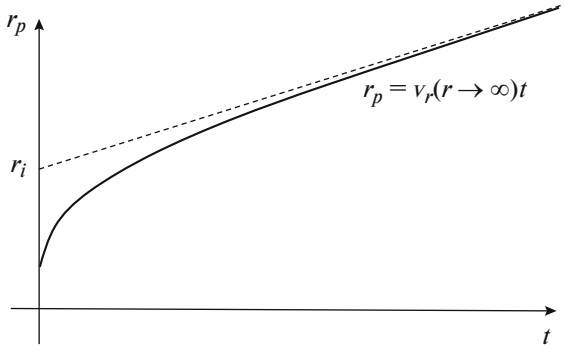

Fig. 10. The expected shell behavior at $\xi > \xi_e$.

Explosion. To explode, the shell must reach $r = \infty$ with at least $\tilde{u}_r = 0$. But as $r \to \infty$, $\sigma \to 0$ and $\phi \to 0$, so that $E^{\text{particle}} \to m$. When the shell is at infinity, E^{field} is a small positive quantity. So for an explosion to happen, the initial energy of the particle-field system must be larger than m,

$$E\Big|_{t=0} > m. \tag{75}$$

In the Newtonian limit $r_i \gg m$, the condition (75) reduces to $\xi > \sqrt{2}$. The escape radial velocity is (see Fig. 10)

$$\tilde{u}_r\Big|_{r\to\infty} = \sqrt{\left[(E\big|_{t=0} - E^{\text{field}}\big|_{t=\infty}/m\right]^2 - 1}$$
$$\approx \sqrt{[E\big|_{t=0}/m]^2 - 1}, \tag{76}$$

or

$$v_r\Big|_{r\to\infty} \approx \frac{\sqrt{E^2\big|_{t=0} - m^2}}{E\big|_{t=0}}. \tag{77}$$

3. APPROXIMATIONS

Here we will describe two approximated solutions of the exact problem stated in Section 2.

3.1. Quasistatic Approximation

When it takes many oscillations for the particle to settle into the final stable circular orbit, we can hope to approximate its slow motion with a quasistatic approximation. The idea is the following. Consider the static version of our problem (Eqs. (14)–(11)),

$$(r\Phi)_{,rr} = \frac{Gme^{2\Phi}}{\tilde{u}^0 r_s} \delta(r - r_s),$$
$$\frac{dr_s}{dt} = \frac{\tilde{u}_r}{\tilde{u}^0},$$
$$\frac{d\tilde{u}_r}{dt} = \frac{\tilde{u}_\phi^2}{\tilde{u}^0 r_s^3} - \frac{e^{2\Phi}\Phi_{,r}}{\tilde{u}^0},$$

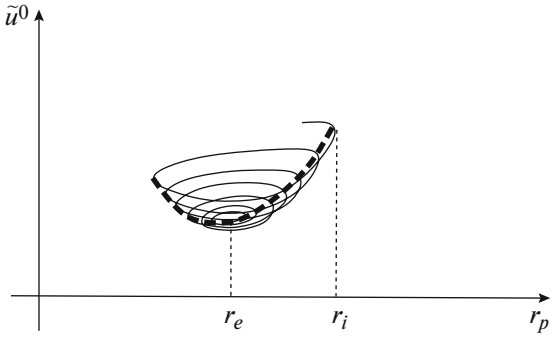

Fig. 11. $\tilde{u}^0$ as a function of the shell radius for the case $\alpha \sim 1$, $\xi < 1$, as expected from exact numerical integration (solid line) and from the analytic expression (81) (dashed line). We expect the dashed curve to pass through the true values of energy at the turning points of the particle orbit.

$$\tilde{u}^0 = \sqrt{e^{2\Phi} + \tilde{u}_r^2 + \tilde{u}_\phi^2/r_s^2}, \quad \tilde{u}_\phi = \text{const}, \qquad (78)$$

where we call $r_s(t)$ the shell radius in this static approximation. At all times, the field must be of the form (20) with $a = a_s$. Once we know $r_s(t)$ and $\tilde{u}_r(t)$, we can determine the field from the jump condition (21)

$$a_s = -\frac{Gm\, e^{2a_s/r_s}}{\sqrt{e^{2a_s/r_s} + \tilde{u}_r^2 + \tilde{u}_\phi^2/r_s^2}}. \qquad (79)$$

Since we have a static field $\Phi = \Phi(r, r_s(t), \tilde{u}_r(t))$, $\Phi_{,t} = 0$, and the system is conservative. The shell will then experience undumped oscillations around its final equilibrium radius r_e. For the shell reach r_e, we need a recipe to dump the oscillations. This will give us a quasistatic approximation to the true shell motion.

Once we know the initial r_i and final r_e shell radii, we can construct a sequence of intermediate "quasistatic" Einstein states as follows. The shell initially at r_i will contract ($\xi < 1$) or expand ($\xi > 1$) towards r_e in a succession of circular orbits ($\tilde{u}_r = 0$) occurring at the true inversion points of the particle trajectory. We call the intermediate radii of these circular orbits, $r_{q.s.}(i) = r_p(P_1 + \ldots + P_i)$, where $P_1, \ldots, P_i$ are the first i oscillation periods. At those points, the field will be of the form (20) with $a = a_{q.s.}$ determined by solving Eq. (21) for any given $r_p = r_{q.s.}(i)$. At each $r_{q.s.}$ we can determine the new value of ξ

$$\xi_{q.s.}(i) = \frac{\tilde{u}_\phi}{e^{a_{q.s.}/r_{q.s.}(i)} r_{q.s.}^2(i) \sqrt{-a_{q.s.}/(2r_{q.s.}^3(i))}}, \qquad (80)$$

the particle energy

$$\tilde{u}^0 = \sqrt{e^{2a_{q.s.}/r_{q.s.}} + \tilde{u}_\phi^2/r_{q.s.}^2}, \qquad (81)$$

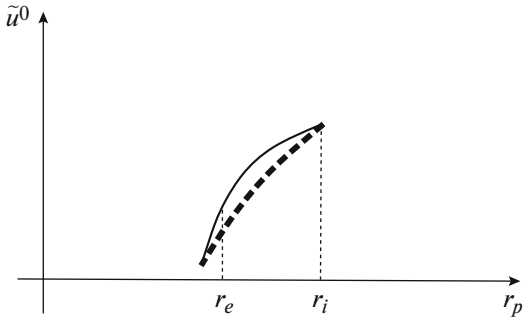

Fig. 12. The same as in Fig. 11 but for $\alpha \gg 1$ and $\xi < 1$.

and the particle-field energy

$$E = \frac{a_{q.s.}^2}{2r_{q.s.}} + m\tilde{u}^0. \qquad (82)$$

We expect this to be a very good approximation for the particle energy at the true inversion points of the particle trajectory for a wide range of α and ξ (see Figs. 11 and 12).

There is usually a value of ξ different from 1, ξ_o, at which the particle energy in the final equilibrium state is equal to its energy at the beginning of the evolution (see Fig. 13). For shells with $\alpha < 0.4204623...$, $\xi_o < 1$, for less compact shells $\xi_o > 1$. One can also show that $E(r_{q.s.})$ has a minimum at $r_{q.s.}(\infty) = r_e$ (see Fig. 14).

Suppose we have approximated the true shell motion up to the i-th period P_i. Then we continue the approximation as follows (see Fig. 15):

1. Calculate $dE/dr_{q.s.}$ from Eq. (82),

$$\frac{dE}{dr_{q.s.}} = -\frac{a_{q.s.}^2}{2r_{q.s.}^2} + \frac{a_{q.s.}^3(5r_{q.s.} - 2a_{q.s.})}{r_{q.s.}(7a_{q.s.}r_{q.s.}^2 - 2a_{q.s.}^2 r_{q.s.} - 4r_{q.s.}^3)} + m\frac{\tilde{u}_\phi^2}{\tilde{u}^0} \times \left(\frac{1}{\xi_{q.s.}^2} \frac{4a_{q.s.} - 8r_{q.s.}}{r_{q.s.}(7a_{q.s.}r_{q.s.}^2 - 2a_{q.s.}^2 r_{q.s.} - 4r_{q.s.}^3)} - \frac{1}{r_{q.s.}^3}\right). \qquad (83)$$

2. Calculate the energy radiated in the i-th oscillation period P_i. In general, if $r > r_p(t)$,

$$\Delta_{P_i} E = \int_{P_1+\ldots+P_{i-1}}^{P_1+\ldots+P_i} dt\, \frac{dE}{dt}, \qquad (84)$$

$$\frac{dE}{dt} = \frac{1}{G} r^2 \Phi_{,t} \Phi_{,r} = -\frac{1}{G}(r\Phi_{,t})^2. \qquad (85)$$

We need a good approximation to the monopole term (the lowest-order contribution to the

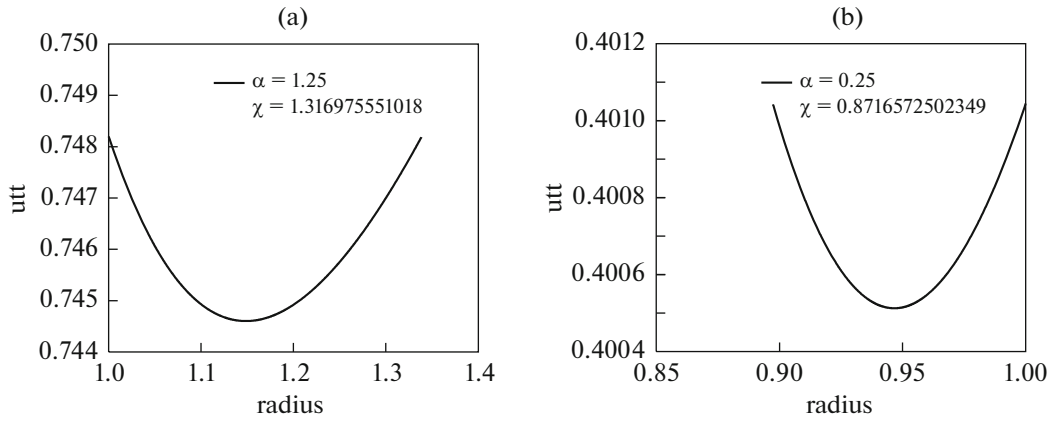

Fig. 13. $\tilde{u}^0$ calculated from Eq. (81) as a function of the shell radius for two different situations: (a) a more compact shell, (b) a less compact one.

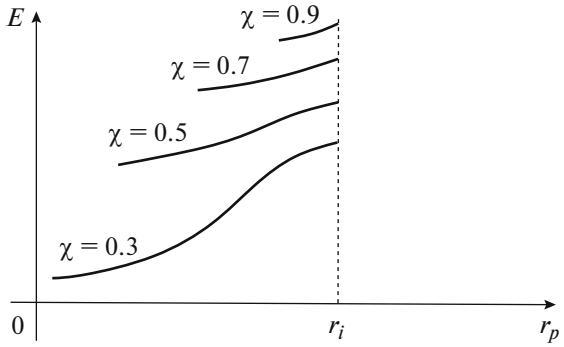

Fig. 14. The expected family of curves for E vs. r_p parametrized by the particle's angular momentum ξ.

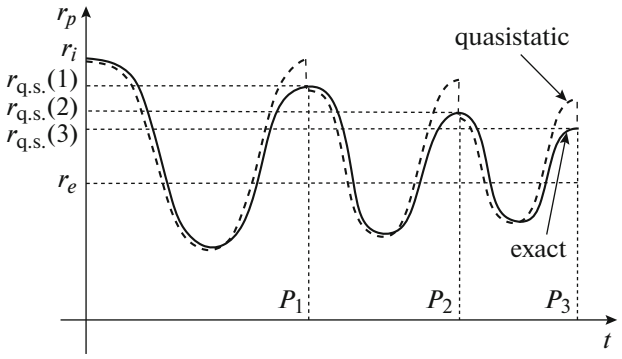

Fig. 15. How the quasistatic approximation is expected to approximate a nonlinear collapse.

radiation) of the wave amplitude $r\Phi(r,t)$. In the weak field, slow motion limit, one finds (see Eq. (49))

$$r\Phi(r,t) = -G\int dr' 4\pi r'^2 \left[\rho_0(\Phi - \tfrac{1}{2}v^2) + \tfrac{1}{6}r_p^2\rho_{0,tt}\right]_{t-r}.$$

If $\alpha \gg 1$, it is sufficient to use the Newtonian approximation. So we will use the analytic expression (63). If $\alpha \sim 1$, we need to use the static approximation (the system (78)) to get a numerical estimate for $\Delta_{P_i}E$. Details of the calculation are outlined in the appendix.

3. Given $r_{q.s.}(i)$ we can find $r_{q.s.}(i+1)$ using the chain rule,

$$r_{q.s.}(i+1) = r_{q.s.}(i) + \frac{\Delta_{P_i}E}{dE/dr_{q.s.}(r_{q.s.}(i))}. \qquad (86)$$

4. Start a new static oscillation from $r_i = r_{q.s.}(i+1)$ and $\xi = \xi_{q.s.}(i+1)$.

3.2. Characteristics Approximation

We adopt a mean-field particle simulation scheme.[4]

1. The particle is evolved in the mean background field Φ for a small time Δt.

2. From the new particle position and velocity we obtain a new matter source term appearing in the field equation (11).

3. We then update Φ by evolving the field equation for a time step Δt.

4. Repeat the whole process.

[4] This scheme resembles Godunov's method used for numerical solution of nonlinear systems of hyperbolic conservation laws [2].

The particle evolves through an ordinary differential equation which poses no computational difficulties. One can, for example, use one of the standard Runge–Kutta schemes. The field evolution is much more problematic. It involves solution of the Cauchy problem for a nonlinear hyperbolic partial differential equation with discontinuous initial data. In the next section we will outline an exact numerical integration scheme for the field equation. Here we will describe an approximate one.

The idea is to use the auxiliary functions $X(r,t)$ and $Y(r,t)$ introduced in Subsection 2.3. We make the following approximation: in the time step dt we evolve the field according to Eq. (26), where we consider the source term F to be constant in time.[5] Under this approximation, given at time t_o, $X(r,t_o) = X_o(r)$, and $Y(r,t_o) = Y_o(r)$ the solutions for X and Y at later times are

$$\begin{aligned} X(r,t) &= X_o(r+\Delta t) - F\,\mathrm{st}[r_p-\Delta t, r_p](r) \\ &\quad + F\,\mathrm{st}[-r_p-\Delta t, -r_p](r), \\ Y(r,t) &= Y_o(r-\Delta t) + F\,\mathrm{st}[r_p, r_p+\Delta t](r) \\ &\quad - F\,\mathrm{st}[-r_p, -r_p+\Delta t](r), \end{aligned} \tag{87}$$

where $\mathrm{st}[a,b](r) = H(x-a) - H(x-b)$ with H the Heaviside function, $\Delta t = t - t_o$, and we added an image source at $r = -r_p(t)$[6] in order to ensure finiteness of the field at the origin at all times, which requires

$$X(0,t) = Y(0,t), \quad \forall t. \tag{88}$$

We then reconstruct the gravitational field as

$$\Phi(r,t) = \frac{1}{r}\int_0^r [X(r,t) + Y(r,t)]\, dr. \tag{89}$$

In our code, we tabulate the field using a uniform grid in r, and we choose $dr = dt$. We need, in fact, to make sure that in using the solutions (87), the source terms fall upon the translated functions less frequently, as possible. Those events are purely due to the mean field scheme, which requires that we move the particle over a fixed field. When $dr = dt$, they occur only when the particle hits a grid point at a given time step.

4. EXACT NUMERICAL INTEGRATION

Here we describe the scheme we use to solve exactly the scalar field equation (11) coupled to the particle equations (14) in spherical symmetry, within the mean-field approximation described in Subsection 3.2.

[5] Note that this is an approximation even within the mean-field scheme since in its definition F contains the field itself.

[6] See Appendix (7) for a justification of our use of the images method in the solution of this particular field equation.

4.1. Characteristics Method

To make the characteristics approximation exact integration, we need to replace the solution (87) with

$$\begin{aligned} X(r,t) &= X_o(r+\Delta t) \\ &\quad - F(r_p, t+(r-r_p))\mathrm{st}[r_p-\Delta t, r_p] \\ &\quad + F(r_p, t+(r+r_p))\mathrm{st}[-r_p-\Delta t, -r_p] \\ Y(r,t) &= Y_o(r+\Delta t) \\ &\quad + F(r_p, t-(r-r_p))\mathrm{st}[r_p-\Delta t, r_p] \\ &\quad - F(r_p, t+(r-r_p))\mathrm{st}[-r_p, -r_p+\Delta t]. \end{aligned} \tag{90}$$

In our numerical integration we have always used the field time step Δt, equal to the particle time step dt, equal to the grid spacing dr. In this case, there is no difference in using Eqs. (90) or (87). If we want to use $\Delta t = ndt$ with $n = 2, 3, \ldots$, then the more general solution (90) should be used and solved by iteration.

4.2. High Resolution Method

A more rigorous method when computing discontinuous solutions of the wave equation can be found among the flux-limiter methods described in chapter 16 of Randall J. LeVeque "Numerical Methods for Conservation Laws". Here we will describe the one employing the "Van Leer" smoother limiter function.

This method is second-order accurate on smooth parts of the field and yet gives a well resolved, nonoscillatory discontinuity at the shell surface (by increasing the amount of numerical dissipation in its neighborhood). The method has the total variation diminishing property provided that the Courant, Friedrichs, and Lewy (CFL) condition is satisfied, and consequently it is mononotonicity preserving.

We will first state the method for a general linear hyperbolic system of partial differential equations and later specialize it to our nonlinear field equation.

Consider the time-dependent Cauchy problem in one space dimension,

$$\begin{gathered} u_{,t} + Au_{,x} = 0, \quad -\infty < x < \infty, \quad t \geq 0, \\ u(x,0) = u_o(x), \end{gathered}$$

where $u \in R^m$, and A is an $n \times n$ matrix. The system is called hyperbolic if A is diagonalizable with real eigenvalues, so that we can decompose $A = R\Lambda R^{-1}$, where $\Lambda = \mathrm{diag}(\lambda_1, \lambda_2 \ldots, \lambda_m)$ is a diagonal matrix of eigenvalues, and $R = [r_1|r_2|\cdots|r_m]$ is the matrix of right eigenvectors of A. Discretize time as $t_n = ndt$ and space as $x_j = jdr$. The finite difference method we want to describe produces approximations $U_j^n \in R^m$ to the solution $u(x_j, t_n) = u_j^n$ at discrete grid points. The method is written in a conservative form as follows:

$$U_j^{n+1} = U_j^n - \frac{dt}{dr}(FL_j^n - FL_{j-1}^n),$$

$$FL_j = FLl_j + FLh_j,$$
$$FLl_j = \frac{1}{2}A(U_j + U_{j+1}) - \frac{1}{2}|A|(U_{j+1} - U_j),$$
$$|A| = R(\Lambda^+ - \Lambda^-)R^{-1},$$
$$\Lambda^\pm = \mathrm{diag}(\lambda_1^\pm, \ldots, \lambda_m^\pm), \quad \lambda_p^\pm = \frac{\max}{\min}(\lambda_p, 0),$$
$$FLh_j = \frac{1}{2}\sum_{p=1}^{m}\phi(\theta_{p_j})(\mathrm{sgn}(\nu_p) - \nu_p)\lambda_p\alpha_{p_j}r_p,$$
$$\nu_p = \lambda_p\frac{dt}{dr},$$
$$\alpha_j = R^{-1}(U_{j+1} - U_j),$$
$$\phi(\theta) = \frac{|\theta| + \theta}{1 + |\theta|},$$

"Van Leer" smoother limiter function,

$$\theta_{p_j} = \frac{\alpha_{p_{j'}}}{\alpha_{p_j}}, \quad j' = j - \mathrm{sgn}\nu_p. \tag{91}$$

FLh is the high order (Lax-Wendroff) flux acting on smooth portions of the solution (where θ is near 1), while FLl is the low-order (first-order upwind) flux acting in the vicinity of a discontinuity (where θ is far from 1). The CFL condition is

$$\left|\frac{\lambda_p dt}{dr}\right| \le 1, \quad \forall p. \tag{92}$$

Our field equation is a wave equation with a nonlinear source term. It can be rewritten as

$$u_{,t} + Au_{,x} = b,$$
$$u = \begin{pmatrix} u1 \\ u2 \end{pmatrix} = \begin{pmatrix} \Psi_{,x} \\ \Psi_{,t} \end{pmatrix}, \quad \Psi(x,t) = x\Phi(x,t),$$
$$A = \begin{pmatrix} 0 & -1 \\ -1 & 0 \end{pmatrix}, \quad |A| = \begin{pmatrix} 1 & 0 \\ 0 & 1 \end{pmatrix},$$
$$\Lambda = \begin{pmatrix} -1 & 0 \\ 0 & 1 \end{pmatrix},$$
$$R = \begin{pmatrix} 1 & 1 \\ 1 & -1 \end{pmatrix}, \quad R^{-1} = \begin{pmatrix} 1/2 & 1/2 \\ 1/2 & -1/2 \end{pmatrix},$$
$$b = \begin{pmatrix} 0 \\ 4\pi G\sigma e^{I_1(x)/x}x[\delta(x-r_p) + \delta(x+r_p)] \end{pmatrix},$$
$$I_1(x) = \int_0^x u1(x',t)dx'. \tag{93}$$

The initial condition is

$$u_o(x) = \begin{pmatrix} -a_i \mathrm{st}[-r_i, r_i](x) \\ 0 \end{pmatrix}. \tag{94}$$

If we call $r_{\max} = j_{\max}dr$ the maximum extent of our grid, the outgoing wave boundary conditions are $\forall t$,

$$u1(x > x_{\max}, t) + u2(x > x_{\max}, t) = 0,$$
$$u1(x < -x_{\max}, t) - u2(x < -x_{\max}, t) = 0. \tag{95}$$

Imagine that we have approximated the true solution of the field equation up to the n-th time slice (i.e., we know U_j^n for $j = -j_{\max}, \ldots, -1, 0, 1, \ldots, j_{\max}$).

The difference scheme,

$$U1_j^{n+1} = f(U1_{j-1}^n, U1_j^n, U1_{j+1}^n, U2_{j-1}^n, U2_j^n, U2_{j+1}^n),$$
$$U2_j^{n+1} = g(U1_{j-1}^n, U1_j^n, U1_{j+1}^n, U2_{j-1}^n, U2_j^n, U2_{j+1}^n),$$

when evaluated at $j_{\max}$, becomes a system of two equations in two unknowns $U1_{j_{\max}}^{n+1}$ and $U1_{j_{\max}+1}^n$,

$$U1_{j_{\max}}^{n+1} = f(U1_{j_{\max}-1}^n, U1_{j_{\max}}^n, U1_{j_{\max}+1}^n, U2_{j_{\max}-1}^n),$$
$$U1_{j_{\max}}^{n+1} = -g(U1_{j_{\max}-1}^n, U1_{j_{\max}}^n, U1_{j_{\max}+1}^n, U2_{j_{\max}-1}^n),$$

allowing the closure of the difference scheme. A consistency check would be to monitor the constraint

$$U2_0^n = 0, \quad \forall n. \tag{96}$$

The difference scheme to be used for the field equation follows from Eq. (91),

$$U_j^{n+1} = U_j^n - \frac{dt}{dr}(FL_j^n - FL_{j-1}^n) + dt\, B_j^n, \tag{97}$$

where B approximates the source term b,

$$B_j^n = \begin{pmatrix} 0 \\ 4\pi G\sigma(t_n)e^{I_1(x_j)/x_j}x_j\frac{\Delta V}{dr} \end{pmatrix}. \tag{98}$$

In Eq. (98), I_1 has been defined in Eq. (93), $\Delta V = W(r_p(t_n) - x_j) - W(-r_p(t_n) - x_j)$, and we have approximated the delta functions using a triangular shaped cloud scheme, which in one dimension employs three mesh points and has an assignment-interpolation function W which is continuous in value and first derivative. The mass is assigned from the particle at r_p to the three mesh points nearest to it,

$$W(x) = \begin{cases} \frac{3}{4} - \left(\frac{x}{dr}\right)^2, & |x| \le \frac{dr}{2} \\ \frac{1}{2}\left(\frac{3}{2} - \frac{|x|}{dr}\right)^2, & \frac{dr}{2} \le |x| \le \frac{3dr}{2} \\ 0 \quad \text{otherwise.} \end{cases} \tag{99}$$

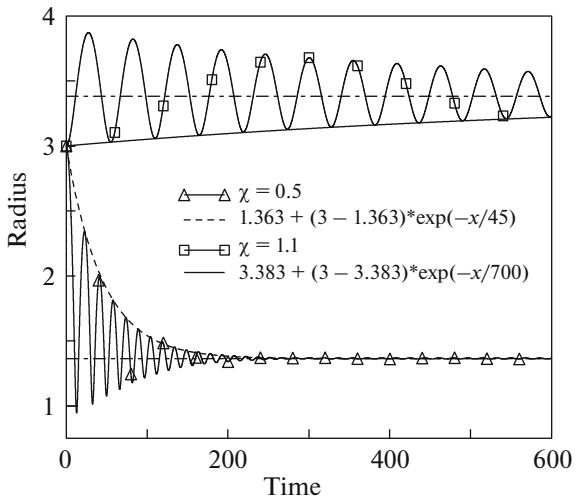

Fig. 16. Relaxation to the virial equilibrium state for an $\alpha = 3$ shell with two different values of ξ. In both cases the decay is fitted well by an exponential.

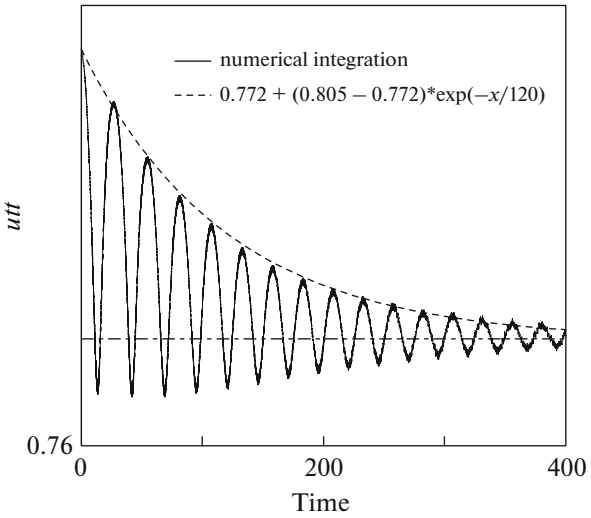

Fig. 17. The particle energy $\tilde{u}^0$ in the case $\alpha = 3, \xi = 0.7$ versus time. The decay to the equilibrium value is well fitted by an exponential.

5. NUMERICAL RESULTS

When analyzing our numerical results, we will adopt gravitational units where $G = c = 1$. In this section, we report the results obtained with the characteristic approximation code (see our supplementary material [3]). We will refer to these results as the "exact integration" results.

5.1. Relaxation to Virial Equilibrium

When trying to reproduce the expected behavior described in Fig. 9, we got Fig. 16.

Trying to reproduce the expected behavior described in Fig. 6 we got Fig. 17.

6. COMPARISON WITH THE ANALYTIC METHOD

We compare numerical integration in the linear and nonlinear regimes with the analytic Newtonian solution.

Monopole radiation. Trying to reproduce the expected behavior described in Fig. 8, we get Fig. 21.

Quasistatic approximation. Trying to reproduce the expected behavior described in Fig. 11, we get Figs. 22 and 23.

7. CONCLUSIONS

In this work, we have developed a toy model for the approach to equilibrium of a spherically symmetric field-particle system initially excited in a non-equilibrium state, where the particle is in an unstable circular orbit around the origin, in the framework of a scalar gravitational field theory [1]. We worked in a quasistatic approximation to the exact dynamical problem of an unstable circular orbit.

In the quest for the gravitational waveform emitted during the inspiral and the final coalescence of two stars, our toy model could give some insights to the full GR physical model, for which the two-body problem is known to be one of the outstanding unsolved problems.

In particular, our method of images approach to the numerical solution of our toy model wave equation (see Appendix 7) has never been used before in the literature.

Some future developments to the present work may be:

0 Correct the characteristics approximation as outlined in Subsection 4.1.

1 Integrate Eqs. (11) and (12) using the finite-difference scheme for the field evolution described in Subsection 4.2.

2 Extend the one-particle problem to a many-particle one, and check how the quasistatic approximation performs there.

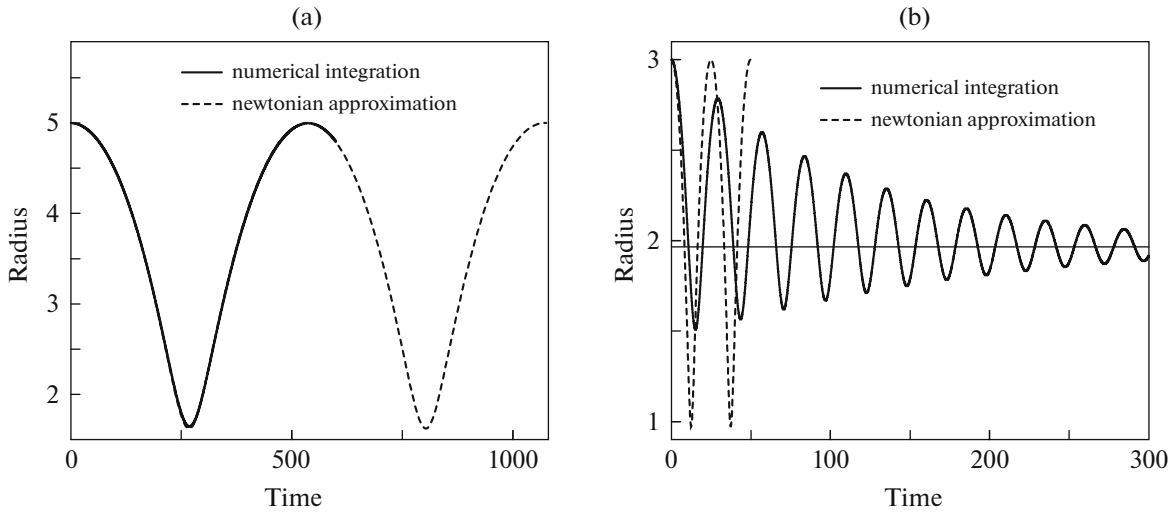

Fig. 18. Comparison of numerical integration with the analytic Newtonian approximation. (a) The quasi-Newtonian $\alpha = 500$, $\xi = 0.7$ shell. The predicted equilibrium radius is at $r_e = 2.4662896500$. (b) The $\alpha = 3$, $\xi = 0.7$ shell. The predicted equilibrium radius is at $r_e = 1.9657627134$.

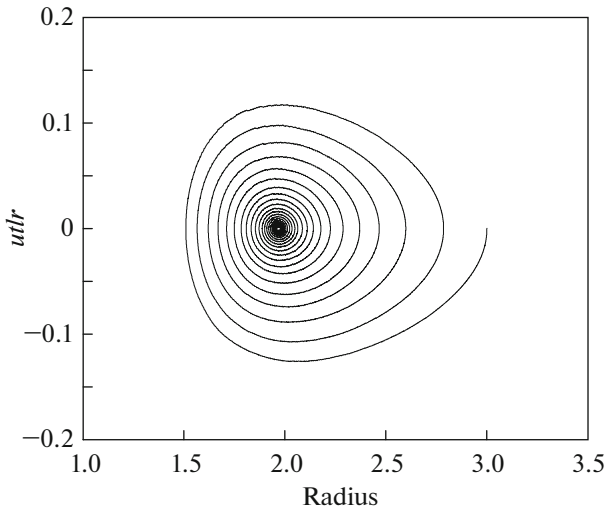

Fig. 19. $\tilde{u}_r$ as a function of the shell radius in the case $\alpha = 3, \xi = 0.7$.

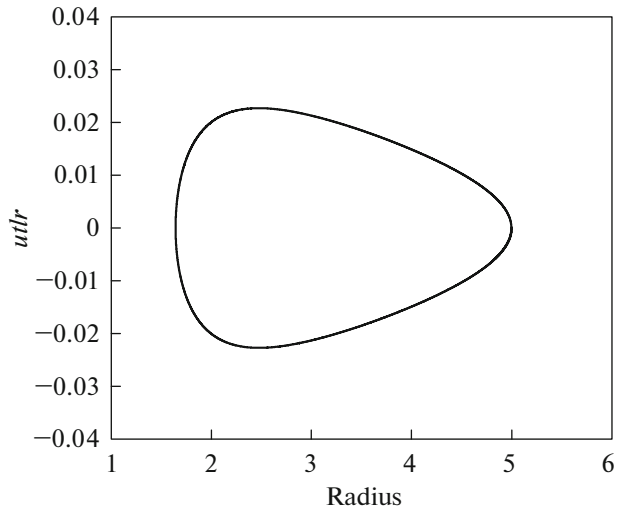

Fig. 20. The same as Fig. 19 for the case $\alpha = 500$, $\xi = 0.7$.

3 Go on to solve more realistic gravitational field theories, and look for quasistatic approximations.

Appendix A

EQUATIONS OF MOTION IN SPHERICAL SYMMETRY

In this Appenix, we derive the equations of motion in spherical symmetry presented in Eq. (14). Spherical symmetry implies $\Phi_{,\theta} = \Phi_{,\phi} = 0$. In spherical coordinates $g_{\alpha\beta} = \mathrm{diag}(-1, 1, r^2, r^2 \sin^2\theta)$, which on the plane $\theta = \pi/2$ becomes $g_{\alpha\beta} = \mathrm{diag}(-1, 1, r^2, r^2)$.

From the definitions $u^\alpha = dz^\alpha/d\tau$, $\tilde{u}^\alpha = e^\Phi u^\alpha$, and $ds^2 = g_{\alpha\beta} dz^\alpha dz^\beta$ immediately follows Eq. (15), where $u^r = u_r$ and $u_\phi = r^2 u^\phi = r^2 u^0 \dot{\phi}$, where the dot is a time derivative, $t = z^0$, as usual, and $u^0 = dt/d\tau = \gamma$, the Lorentz factor.

Note that $Du^\alpha/dt = u^\alpha{}_{;0} = \dot{u}^\alpha + u^\mu \Gamma^\alpha{}_{\mu 0}$, where the only nonzero Christoffel symbol is $\Gamma^\phi{}_{\phi 0} = \dot{r}/r = \tilde{u}^r/r\tilde{u}^0$.

From the particle equation of motion (12) we find

$$u^0 u^\alpha_{;0} + \Phi_,{}^\alpha + u^\alpha(u^r \Phi_{,r} + u^0 \Phi_{,0}) = 0. \qquad \text{(A.1)}$$

We then find

$$\dot{\tilde{u}}^\phi = e^\Phi \Phi_{,0} u^\phi + e^\Phi \dot{u}^\phi = -\frac{\tilde{u}^\phi \tilde{u}^r}{\tilde{u}^0 r} - \frac{\tilde{u}^\phi \tilde{u}^r}{\tilde{u}^0} \Phi_{,r}, \qquad \text{(A.2)}$$

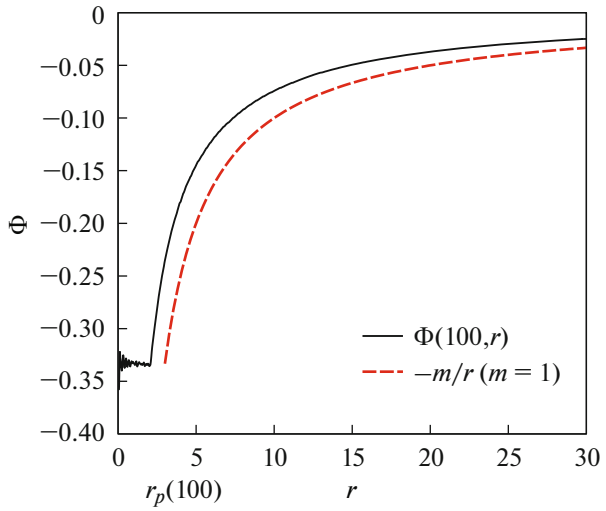

Fig. 21. A snapshot at $t = 100$ of the field $\Phi(100, t)$ in the case $\alpha = 3$, $\xi = 0.7$, and the zeroth order radiation part $-m/r$.

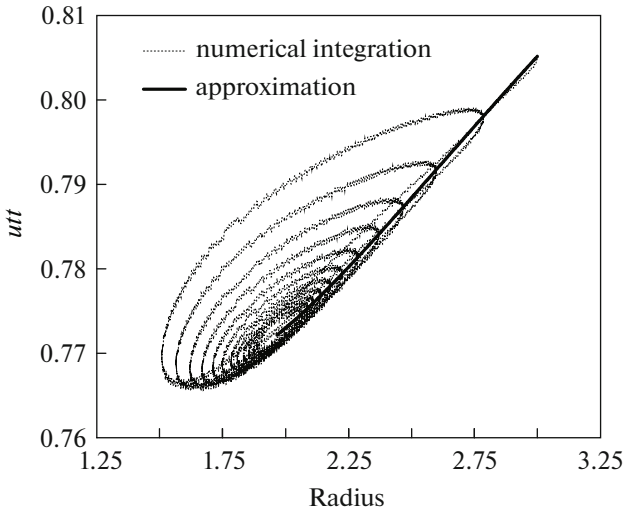

Fig. 22. $\tilde{u}^0$ as a function of the shell radius for numerical integration in the case $\alpha = 3$, $\xi = 0.7$. The solid line was derived using the analytic expression (81). We see that it approximates well the values of energy at the turning points.

$$\dot{\tilde{u}}^r = e^{\Phi}\Phi_{,0}u^r + e^{\Phi}\dot{u}^r = -\frac{e^{2\Phi}\Phi_{,r}}{\tilde{u}^0} - \frac{\tilde{u}_r^2}{\tilde{u}^0}\Phi_{,r}, \quad \text{(A.3)}$$

so that, since $\tilde{u}_\phi = r^2\tilde{u}^\phi$, we have

$$\dot{\tilde{u}}_\phi = 2r\dot{r}\tilde{u}^\phi + r^2\dot{\tilde{u}}^\phi$$
$$= r\frac{\tilde{u}^\phi\tilde{u}^r}{\tilde{u}^0} - r^2\frac{\tilde{u}^\phi\tilde{u}^r}{\tilde{u}^0}\Phi_{,r} = 0, \quad \text{(A.4)}$$

where in the last equality we used the fact that in the reference frame of the particle the scalar gravitational field Φ is static, so that its equation (11) on the $\theta = \pi/2$ plane becomes

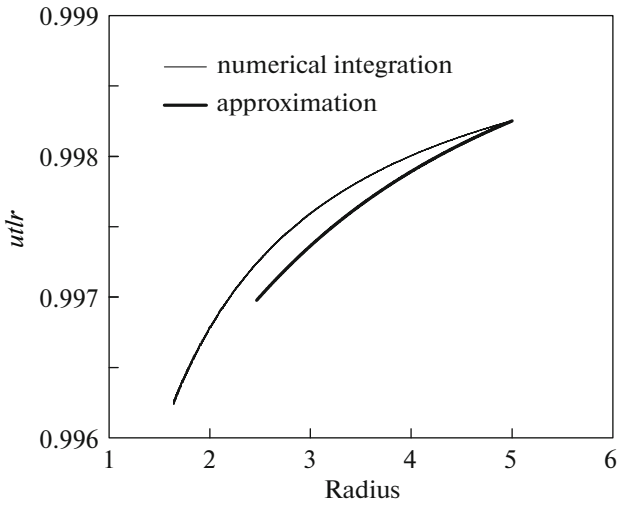

Fig. 23. The same as in Fig. 11 but for $\alpha = 500$, $\xi = 0.7$.

$$\frac{1}{r}\left(r\Phi_{,r}\right)_{,r} = -2\pi\delta^2(\mathbf{z}), \quad \text{(A.5)}$$

which has the solution $\Phi(r) = \ln r$. Then we conclude that the particle's "orbital angular momentum" $\tilde{u}_\phi$ is conserved.

On the other hand, since $\tilde{u}_r = \tilde{u}^r$, we find from Eq. (A.3)

$$\dot{\tilde{u}}_r = -\frac{e^{2\Phi}\Phi_{,r}}{\tilde{u}^0} - \frac{(\tilde{u}_r)^2}{\tilde{u}^0}\Phi_{,r}$$
$$= -\frac{e^{2\Phi}\Phi_{,r}}{\tilde{u}^0} + \frac{(\tilde{u}_r)^2}{r\tilde{u}^0}. \quad \text{(A.6)}$$

In the comoving frame $d\tau = dt$, so that $rd\phi = -dr$, and $ru^\phi = -u^r$ or $(1/r)u_\phi = -u^r$, and we find

$$\dot{\tilde{u}}_r = -\frac{e^{2\Phi}\Phi_{,r}}{\tilde{u}^0} + \frac{(\tilde{u}_\phi)^2}{r^3\tilde{u}^0}. \quad \text{(A.7)}$$

Appendix B

ENERGY LOSS IN THE STATIC APPROXIMATION

In the weak field, slow motion limit, in the wave zone the gravity wave amplitude can be written (dropping terms higher than the monopole ones) as (see Eq. (49) in the main text)

$$r\Phi(r,t) = -G\int dr'\,4\pi r'^2[\rho_0(\Phi - \tfrac{1}{2}v^2)$$
$$+ \tfrac{1}{6}r_p^2\rho_{0,tt}]_{t-r},$$

where in the static approximation

$$\rho_o = \frac{m}{4\pi r_s^2}\delta(r' - r_s),$$

$$v^2 = (\dot{r}_s)^2 + \left(\frac{\tilde{u}_\phi}{\tilde{u}^0}\right)^2 \frac{1}{r_s^2},$$

$$\Phi = \begin{cases} a_s/r_s, & r \le r_s \\ a_s/r, & r > r_s, \end{cases} \tag{B.1}$$

and $a_s = a_s(r_s, \tilde{u}_r)$ through the jump condition (see Eq. (79) in the main text),

$$a_s = -\frac{Gm\, e^{2a_s/r_s}}{\sqrt{e^{2a_s/r_s} + \tilde{u}_r^2 + \tilde{u}_\phi^2/r_s^2}}.$$

Then we can rewrite the wave amplitude as follows:

$$\begin{aligned} r\Phi(r,t) &= -Gm\Bigg\{\frac{a_s}{r_s} - \frac{(\dot{r}_s)^2}{2} - \left(\frac{\tilde{u}_\phi}{\tilde{u}^0}\right)^2 \frac{1}{2r_s^2} \\ &\quad + \frac{1}{3}[(\dot{r}_s)^2 + r_s\ddot{r}_s]\Bigg\}_{t-r}, \\ &= -Gm\Bigg\{\frac{a_s}{r_s} - \left(\frac{\tilde{u}_\phi}{\tilde{u}^0}\right)^2 \frac{1}{2r_s^2} \\ &\quad - \frac{1}{6}(\dot{r}_s)^2 + \frac{1}{3}r_s\ddot{r}_s\Bigg\}_{t-r}. \end{aligned} \tag{B.2}$$

Taking a time derivative, one gets (both $\tilde{u}^0$ and $\tilde{u}_\phi$ are constants of motion),

$$\begin{aligned} r\Phi_{,t} &= -Gm\Bigg\{\frac{\dot{a}_s}{r_s} - \frac{a_s\dot{r}_s}{r_s^2} \\ &\quad + \left(\frac{\tilde{u}_\phi}{\tilde{u}^0}\right)^2 \frac{\dot{r}_s}{r_s^3} + \frac{1}{3}r_s\dddot{r}_s\Bigg\}_{t-r}. \end{aligned} \tag{B.3}$$

In the static approximation,

$$\dot{r}_s = \frac{\tilde{u}_r}{\tilde{u}^0},$$

$$\ddot{r}_s = \frac{\dot{\tilde{u}}_r}{\tilde{u}^0} = \left(\frac{\tilde{u}_\phi}{\tilde{u}^0}\right)^2 \frac{1}{r_s^3} - \frac{e^{2a_s/r_s}}{(\tilde{u}^0)^2}\frac{a_s}{2r_s^2},$$

$$\begin{aligned} \dddot{r}_s &= -\left(\frac{\tilde{u}_\phi}{\tilde{u}^0}\right)^2 \frac{3\dot{r}_s}{r_s^4} - \frac{e^{2a_s/r_s}}{2(\tilde{u}^0)^2}\left(\frac{\dot{a}_s}{r_s^2} - \frac{2a_s\dot{r}_s}{r_s^3}\right) \\ &\quad - \frac{e^{2a_s/r_s}}{(\tilde{u}^0)^2}\frac{a_s}{r_s^2}\left(\frac{\dot{a}_s}{r_s} - \frac{a_s\dot{r}_s}{r_s^2}\right), \end{aligned}$$

$$\dot{a}_s = (a_s)_{,\tilde{u}_r}\tilde{u}^0\ddot{r}_s + (a_s)_{,r_s}\dot{r}_s,$$

$$(a_s)_{,\tilde{u}_r} = -\frac{\tilde{u}_r \frac{a}{e^{2a_s/r_s} + \tilde{u}_r^2 + \tilde{u}_\phi^2/r_s^2}}{1 - \frac{2a_s}{r_s} + \frac{a_s}{r_s}\frac{e^{2a_s/r_s}}{e^{2a_s/r_s} + \tilde{u}_r^2 + \tilde{u}_\phi^2/r_s^2}},$$

$$(a_s)_{,r_s} = -\frac{\frac{2a_s^2}{r_s^2} - \frac{a_s^2}{r_s^2}\frac{e^{2a_s/r_s}}{e^{2a_s/r_s} + \tilde{u}_r^2 + \tilde{u}_\phi^2/r_s^2}}{1 - \frac{2a_s}{r_s} + \frac{a_s}{r_s}\frac{e^{2a_s/r_s}}{e^{2a_s/r_s} + \tilde{u}_r^2 + \tilde{u}_\phi^2/r_s^2}}. \tag{B.4}$$

Using Eqs. (B.4)–(B.4) in Eq. (B.3), one can determine numerically the rate of energy loss (53). This can then be integrated to get the energy emitted by the particle in a full revolution around the origin. This calculation can be carried out analytically in the Newtonian approximation, as we will now shown in detail.

Newtonian approximation. In this approximation we have

$$a_s \to -Gm, \tag{B.5}$$

$$\frac{\tilde{u}_\phi}{\tilde{u}^0} \to \sqrt{\frac{Gm\xi^2 r_i}{2}}, \tag{B.6}$$

$$\ddot{r}_s \to -\frac{Gm}{2r_s^2} + \frac{Gm\xi^2 r_i}{2r_s^3}. \tag{B.7}$$

Making these substitutions in Eq. (B.3), we get Eq. (61) of the main text,

$$r\Phi_{,t} = -\frac{4}{3}\frac{(Gm)^2}{r_i}\left[\frac{\dot{x}}{x^2}\right]_{t-r}, \tag{B.8}$$

where $x = r_s/r_i$. So for the energy emission rate in the wave zone we get Eq. (62), which, integrated over one orbital period, gives Eq. (63).

Appendix C

METHOD OF IMAGES

We want to justify making use of the images method in the solution of the nonlinear field equation (11).

To do that, we need to show the equivalence between the following two problems. Calling $\Psi(r,t) = r\Phi(r,t)$, with $r \in [0,\infty]$, the first problem (problem 1) is our original one, namely,

$$\begin{cases} \Psi_{,tt} - \Psi_{,rr} = F(r,\Psi(r,t))\delta(r - r_p) \\ \Psi(r,0) = f(r), \quad \text{i.c.} \\ \Psi_{,t}(r,0) = 0, \quad \text{i.c.} \\ \Psi(0,t) = 0, \quad \text{b.c.} \\ \Psi_{,r}(r_m,t) + \Psi_{,t}(r_m,t) = 0, \quad \text{b.c.}, \end{cases} \tag{C.1}$$

where i.c. stands for initial conditions and b.c. for boundary conditions.

The second problem (problem 2) is over the whole real axis, $x \in [-\infty,\infty]$, and employs two sources, the one at r_p, of the first problem, and its image,

$$\begin{cases} \Psi_{,tt} - \Psi_{,xx} = F(x,\Psi(x,t)) \\ \quad \times[\delta(x - r_p) + \delta(x + r_p)] \\ \Psi(x,0) = f(x) - f(-x), \quad \text{i.c.} \\ \Psi_{,t}(x,0) = 0, \quad \text{i.c.} \\ \Psi_{,x}(\pm r_m,t) \pm \Psi_{,t}(\pm r_m,t) = 0, \quad \text{b.c.} \end{cases} \tag{C.2}$$

The general solution to problem 1 can be written in an integral form as follows:

$$\Psi(r,t) = \frac{1}{2}[f(r+t) + f(r-t) + W_{r_p}(r,t)] - \frac{1}{2}[r \to -r], \tag{C.3}$$

where

$$W_{r_p}(r,t) = \int_0^t d\overline{t}\, F(r_p, \Psi(r_p,t))[H(r_p - r + (t-\overline{t})) - H(-r_p + r + (t-\overline{t}))], \tag{C.4}$$

and the last term in Eq. (C.3) was added in order for the solution to satisfy the boundary condition at $r = 0$. The outgoing wave boundary condition is automatically satisfied since r_m is intended to be at all times to the right of the source, and $f(r)$ is constant at $r > r_p(0)$. So there are no ingoing waves passing through r_m.

The general solution to problem 2 can be written in integral form as follows:

$$\Psi(r,t) = \frac{1}{2}\Big\{[f(x+t) - f(-x-t)] + [f(x-t) - f(-x+t)] + W_{r_p}(x,t) + W_{-r_p}(x,t)\Big\}. \tag{C.5}$$

For the two problems to have the same solution at $x \geq 0$, the following condition must be satisfied:

$$W_{r_p}(-x,t) = -W_{-r_p}(x,t). \tag{C.6}$$

This condition is equivalent to

$$F(r_p, \Psi(r_p,t)) = -F(-r_p, \Psi(-r_p,t)) = -F(-r_p, -\Psi(r_p,t)), \tag{C.7}$$

where in the last equality we used the fact that the field is an odd function of x at all times. We can easily verify that our field equation, where

$$F(r_p, \Psi(r_p,t)) = -\frac{Gm}{r_p} \times \frac{e^{2\Psi(r_p,t)/r_p}}{\sqrt{e^{2\Psi(r_p,t)/r_p} + \tilde{u}_r^2 + \tilde{u}_\phi^2/r_p^2}}, \tag{C.8}$$

satisfies this condition.

Appendix D

THE INHOMOGENEOUS WAVE EQUATION

We want to find a solution to the following problem:

$$\Psi_{,tt} - \Psi_{,xx} = F(x,t), \tag{D.1}$$

$$\Psi(x,0) = 0, \tag{D.2}$$

$$\Psi_{,t}(x,0) = 0. \tag{D.3}$$

Make the substitution

$$\xi = x + t, \quad \eta = x - t. \tag{D.4}$$

The differential equation then becomes

$$\Psi_{,\xi\eta}\left(\frac{\xi+\eta}{2}, \frac{\xi-\eta}{2}\right) = -\frac{1}{4}F\left(\frac{\xi+\eta}{2}, \frac{\xi-\eta}{2}\right). \tag{D.5}$$

Integrating with respect to ξ, we obtain

$$\Psi_{,\eta}\left(\frac{\xi+\eta}{2}, \frac{\xi-\eta}{2}\right) = .\Psi_\eta\left(\frac{\xi+\eta}{2}, \frac{\xi-\eta}{2}\right)\Big|_{\overline{\xi}=\eta} + \int_\eta^\xi \Psi_{,\xi\eta}\left(\frac{\overline{\xi}+\eta}{2}, \frac{\overline{\xi}-\eta}{2}\right) d\overline{\xi} = \frac{1}{2}\Psi_{,x}(\eta,0) - \frac{1}{2}\Psi_{,t}(\eta,0) - \frac{1}{4}\int_\eta^\xi F\left(\frac{\overline{\xi}+\eta}{2}, \frac{\overline{\xi}-\eta}{2}\right) d\overline{\xi}. \tag{D.6}$$

We integrate this equation from an arbitrary value of η to ξ to find

$$\Psi(\xi,0) - \Psi\left(\frac{\xi+\eta}{2}, \frac{\xi-\eta}{2}\right) = \int_\eta^\xi \left[\frac{1}{2}\Psi_{,x}(\overline{\eta},0) - \frac{1}{2}\Psi_{,t}(\overline{\eta},0)\right] d\overline{\eta} - \frac{1}{4}\int_\eta^\xi \int_{\overline{\eta}}^\xi F\left(\frac{\overline{\xi}+\overline{\eta}}{2}, \frac{\overline{\xi}-\overline{\eta}}{2}\right) d\overline{\xi} d\overline{\eta}. \tag{D.7}$$

In the first integral we note that

$$\int_\eta^\xi \Psi_{,x}(\overline{\eta},0) d\overline{\eta} = \Psi(\xi,0) - \Psi(\eta,0). \tag{D.8}$$

In the second integral we let

$$\overline{\eta} = \overline{x} - \overline{t}, \quad \overline{\xi} = \overline{x} + \overline{t}. \tag{D.9}$$

The integration domain $\eta \le \overline{\eta} \le \overline{\xi} \le \xi$ becomes

$$\eta \le \overline{x} - \overline{t} \le \overline{x} + \overline{t} \le \xi, \tag{D.10}$$

or

$$\eta + \overline{t} \le \overline{x} \le \xi - \overline{t}, \quad 0 \le \overline{t} \le \frac{1}{2}(\xi - \eta). \tag{D.11}$$

The Jacobian determinant of the transformation from $(\overline{\xi}, \overline{\eta})$ to $(\overline{x}, \overline{t})$ is 2. Therefore,

$$\begin{aligned} &\frac{1}{4}\int_{\eta}^{\xi}\int_{\overline{\eta}}^{\xi} F\left(\frac{\overline{\xi}+\overline{\eta}}{2}, \frac{\overline{\xi}-\overline{\eta}}{2}\right) d\overline{\xi} d\overline{\eta} \\ &= \frac{1}{2}\int_{0}^{(\xi-\eta)/2}\int_{\eta+\overline{t}}^{\xi-\overline{t}} F(\overline{x}, \overline{t}) d\overline{x} d\overline{t}. \end{aligned} \tag{D.12}$$

Making these substitutions and transposing, we find

$$\begin{aligned} \Psi\left(\frac{\xi+\eta}{2}, \frac{\xi-\eta}{2}\right) &= \frac{1}{2}[\Psi(\xi, 0) + \Psi(\eta, 0)] \\ &+ \frac{1}{2}\int_{\eta}^{\xi} \Psi_{,t}(\overline{x}, 0) d\overline{x} \\ &+ \frac{1}{2}\int_{0}^{(\xi-\eta)/2}\int_{\eta+\overline{t}}^{\xi-\overline{t}} F(\overline{x}, \overline{t}) d\overline{x} d\overline{t}. \end{aligned} \tag{D.13}$$

We recall that $\xi = x + t$ and $\eta = x - t$ and use the initial conditions to obtain the solution formula

$$\Psi(x, t) = \frac{1}{2}\int_{0}^{t}\int_{x-(t-\overline{t})}^{x+(t-\overline{t})} F(\overline{x}, \overline{t})\, d\overline{x}\, d\overline{t}. \tag{D.14}$$

FUNDING

This work was supported by ongoing institutional funding. No additional grants to carry out or direct this particular research were obtained.

CONFLICT OF INTEREST

The author of this work declares that he has no conflicts of interest.

REFERENCES

1. S. L. Shapiro and S. A. Teukolsky, "Scalar gravitation: A laboratory for numerical relativity," Phys. Rev. D **47**, 1529 (1992).
2. S. K. Godunov, "A finite difference method for the numerical computation of discontinuous solutions of the equations of fluid dynamics," Mat. Sb. **47**, 271 (1959).
3. The supplementary material with the FORTRAN code listing can be found at https://rfantoni.github.io/personal-page/publications/sm-scalarg.pdf.